Methods and optimisation for OBACHT lighting

H. Steel[1], A. Navitski[1]

July 21, 2015

Abstract

Due to the highly reflective nature of the inner surface of niobium superconducting cavities, imaging methods require a careful approach to lighting, such that a uniformly lit picture can be produced whilst maintaining the ability to distinguish fine surface features. For the OBACHT setup this is implemented by means of an adaptable strip lighting setup installed around the camera's aperture, as well as small LED's installed behind the semi-transparent imaging mirror. Two main difficulties persist; when imaging normal to the surface of the cavity, a large poorly-lit band (corresponding to the reflection of the camera itself) is present, and when all lights are illuminated, the near-uniform lighting can wash out fine features of the surface. In this report the causes of these issues are analysed, and potential solutions are established, which include imaging surfaces from an angle, and an image-combination algorithm for superior lighting.

[1] DESY, Hamburg, Germany

1 Introduction

Currently installed on the OBACHT [1, 2] are 21 curved LED illumination strips, numbered from -10 to +10 (figure 1). Strip number zero has a hole cut from the centre, through which light travels (via an angle-adjustable semi-transparent mirror) to the camera. In addition to the strip lights, there are three LEDs behind the semi-transparent mirror, which provide light in an attempt to compensate for that missing due to the camera's viewing hole. The LED strips are mounted on a sliding clamp, for which movement is coupled to the mirror's orientation. This allows transverse alignment of the viewing window to maintain line of sight between the camera and cavity surface when the mirror's angle is changed.

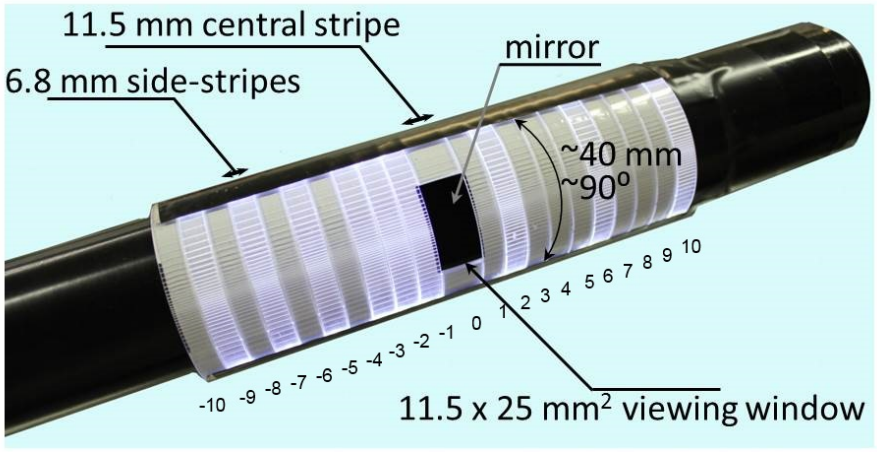

Figure 1: Lighting available at OBACHT, comprising of 21 LED strips and three small LEDs positioned behind the semi-transparent mirror.

Each of the LED strips can be turned off/on individually, via a control panel (figure 2) or software, and their collective intensity (i.e. not individual intensity) can be adjusted.

Figure 2: Lighting control panel for OBACHT. Each LED strip can be activated individually, and their collective intensity adjusted. The central light, comprising three white LEDs behind the semi-transparent mirror, can have its intensity adjusted independently.

Weaknesses in this lighting system arise from two main causes:
First, when images are captured normal to a surface, the reflection of the camera presents a dark vertical band/s in the image (figure 3(a), (b), and (d)), as the camera itself is not a light source. The LEDs positioned behind the semi-transparent mirror are designed to counteract this effect, however, they are not able to eliminate it due to their inability to provide a suitably

diffuse light source emanating from all areas of the tube's dark interior. Their contribution is visible in figure 3(a) and (b) as bright white highlights in the three dark vertical bands.

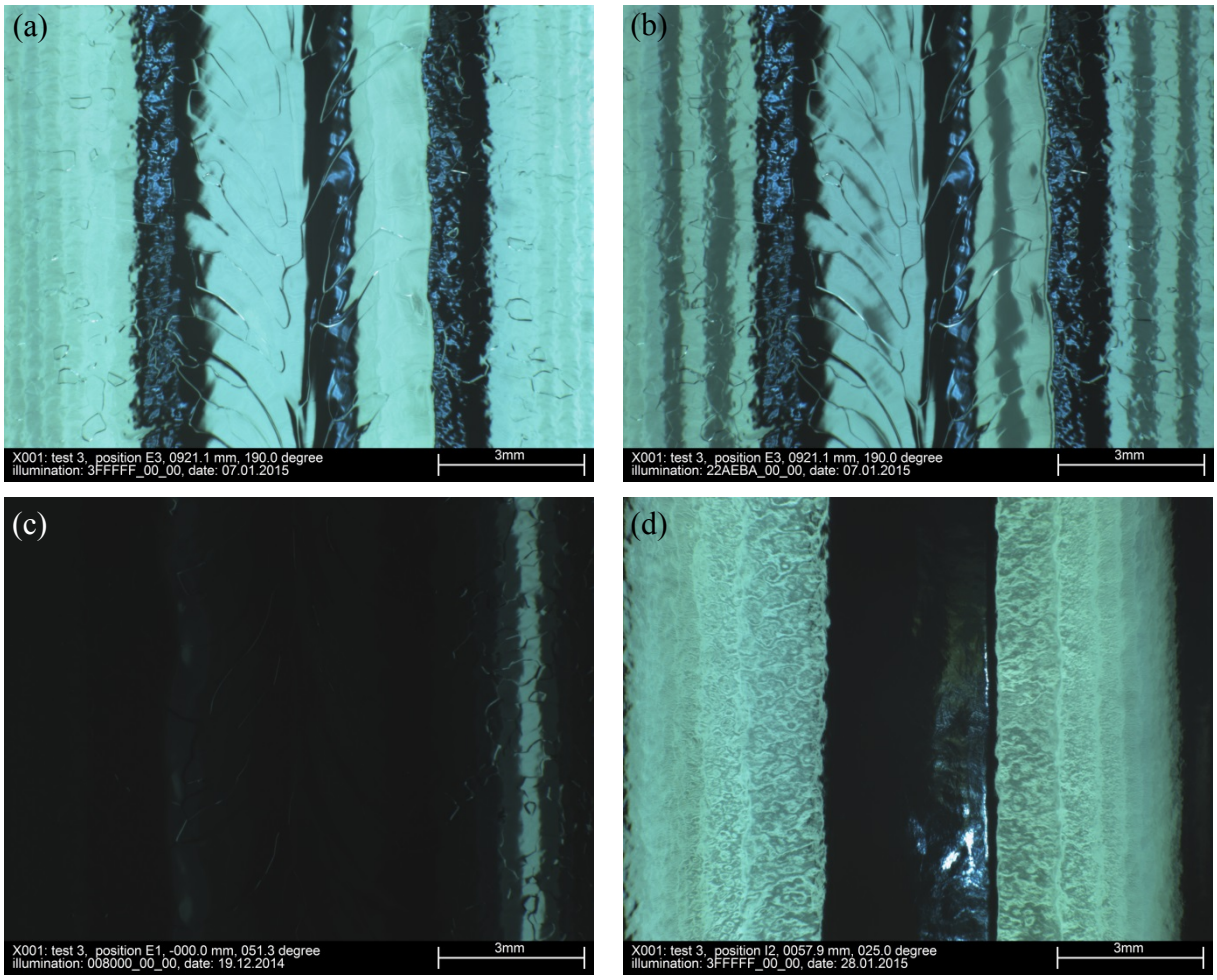

Figure 3: Lighting distribution for OBACHT: a) equatorial image with all illumination activated (hexadecimal code 3FFFFF), displaying three dark bands; b) current best-case illumination (hexadecimal code 23CD78), by deactivating some strips the finer details of the image are not washed out; c) the effect of a single LED strip at the equator, in this case strip # 5; and d) iris image with all illumination, displaying dark central band.

The second difficulty in imaging arises (predominantly for equatorial images) when all illumination strips are activated. This would in some ways be the ideal lighting arrangement, as a uniform lighting intensity across the image is desirous for automated image analysis techniques, however, when this is done the scene is so uniformly lit that shadows cast by the edges of surface features are minimised, making them tough to see (figure 3(a)). Currently, a compromise is used (figure 3(b)), which involves deactivating an experimentally determined set of LEDs, resulting in greater shadowing and hence visibility of surface features, but at the expense of introducing a number of darker vertical bands.

2 Analysis of Lighting Distributions

2.1 Equatorial Lighting Distribution

Based on ray tracing arguments, we can assess how each individual light source contributes to an overall image taken at the equator. Figure 4 shows the cross-sectional profile of a typical welding steam, acquired via laser microscopy of a silicone surface replica [2], which is assumed to be constant in the image's vertical direction. The geometry of the cavity, which would ideally present a perfectly circular cross section at the equator, is clearly distorted in the presence of the welding seam. A small hump emerges in the centre of the seam, and a depression is formed on each side of this in the heat-affected zone. From this shape ray-tracing can be performed to explain the effect of each source on the resultant picture.

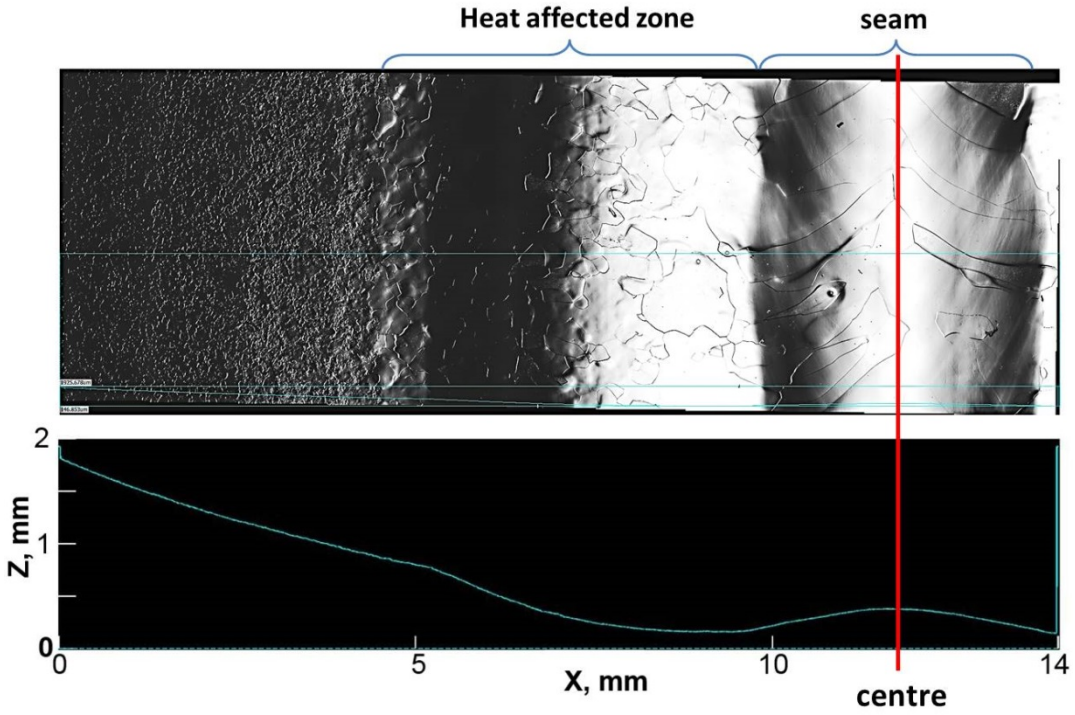

Figure 4: Cross sectional geometry of a typical cavity equator, acquired via laser microscopy of a silicone surface replica.

In figure 5, the lighting arrangement that results from activating a single LED strip light near to the camera hole is demonstrated. It is observed that two reflections are generated, and both reflections move towards the edges of the image (outwards) for light number -2 when compared to -1. The mechanism for this is shown in figure 6, where the ray tracing demonstrates that this lighting arrangement is a consequence of the surface profile.
The ray from each light is reflected from two locations (figure 6). First, it is reflected from the surface below it, as would be expected if the cell surface was a plane mirror. The second reflection is due to curvature of the surface, and requires the ray to travel past the location of the camera, then reflect backward, hence producing reflections in the opposite order.

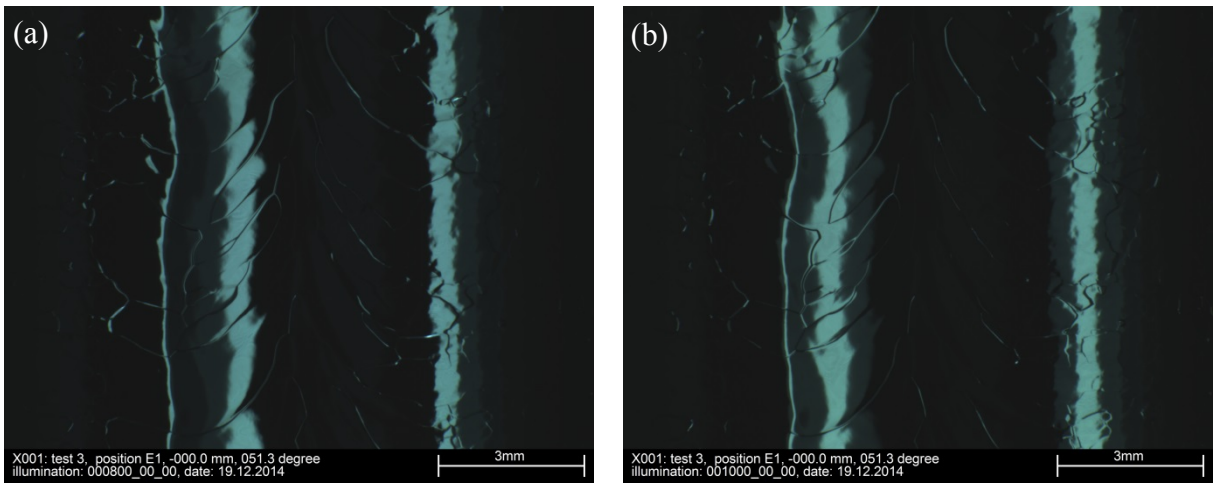

Figure 5: Welding seam lit with a) strip LED # -1 and b) strip LED # -2. In b) both bright bands have moved towards the edges of the image.

As the light source moves further from the camera, there eventually comes a point where the slope of the depression next to the welding seam is not great enough to reflect the LED strip back to the camera's aperture. This is shown in figure 7, where Strip LED #-4 is just on the verge of not being reflected, and strip #-5 is now too far away (or to put it differently, the slope of the cavity's profile is not great enough) to allow the left hand reflection to reach the camera. Ray tracing for this situation (figure 6) demonstrates how this takes place, and reveals why the order of the lights is reversed between the two reflection locations.

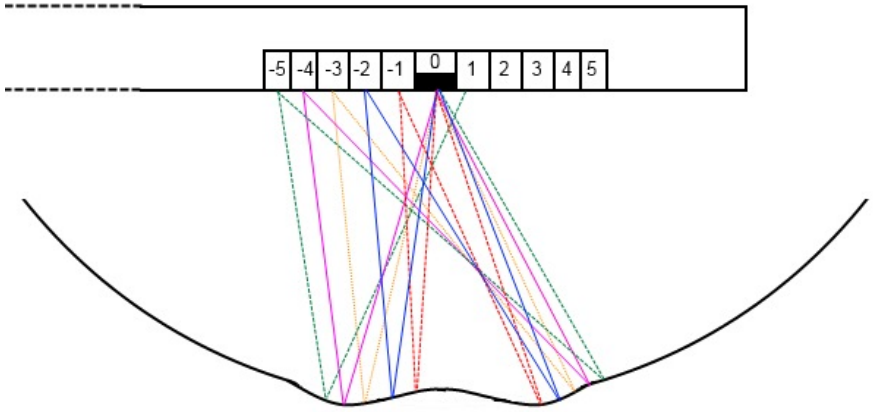

Figure 6: Ray tracing (not to scale) for LEDs # -1 to -5. LED -4 is just able to be reflected from the left of the image back to the camera, whilst -5 is no longer able to reach the camera's aperture, and hence is visible only in the right side reflection. Angles and distances have been exaggerated significantly for demonstrative purposes.

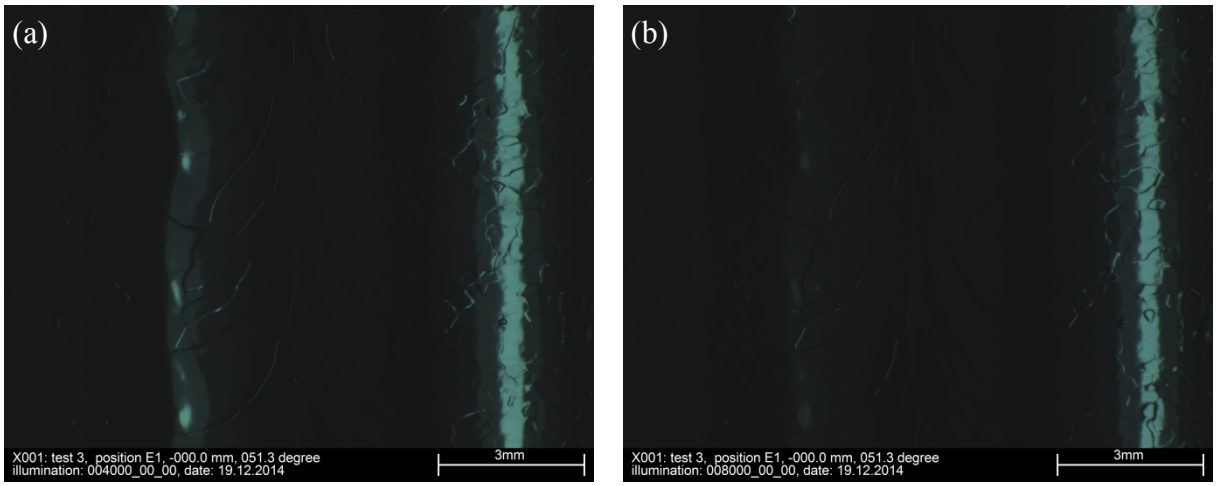

Figure 7: Welding seam lit with a) strip LED # -4 and b) Strip LED # -5. The left hand reflection is barely visible in a) and essentially gone in b).

The three dark stripes observed in images where all illumination is activated are a result of the camera seeing it self, hence appear dark as the camera presents no light source. The LED's behind the semi-transparent mirror are meant to combat this, but do not provide the required intensity, resulting in weak illumination in the regions of aperture reflection. The cavity seam geometry therefore generally results in three black stripes being seen (figure 8).

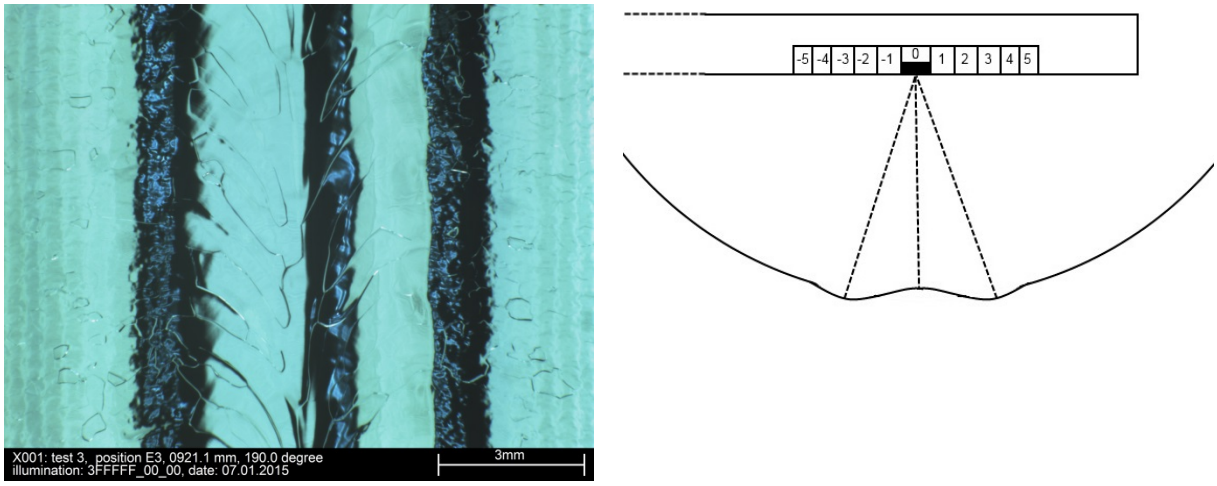

Figure 8: With all lights activated, the cavity geometry results in three reflections of the camera aperture, giving three vertical dark bands.

2.2 Cell Lighting Distribution

Lighting at the cell location of the cavity (next to the welding seam) presents complications due to surface geometry in the same way as at the equator. The camera's limited field of view means only contributions from (for the cell side with the equator to the left of the image, as in figure 9 LED #-10 through #-4 are visible. The contribution from light #-10 appears almost as a single bright band in the centre (figure 9(b)), and as we sequentially move to the next strips # (-9, -8, -7 …) two reflections are formed which move outwards (figure 9(a)).

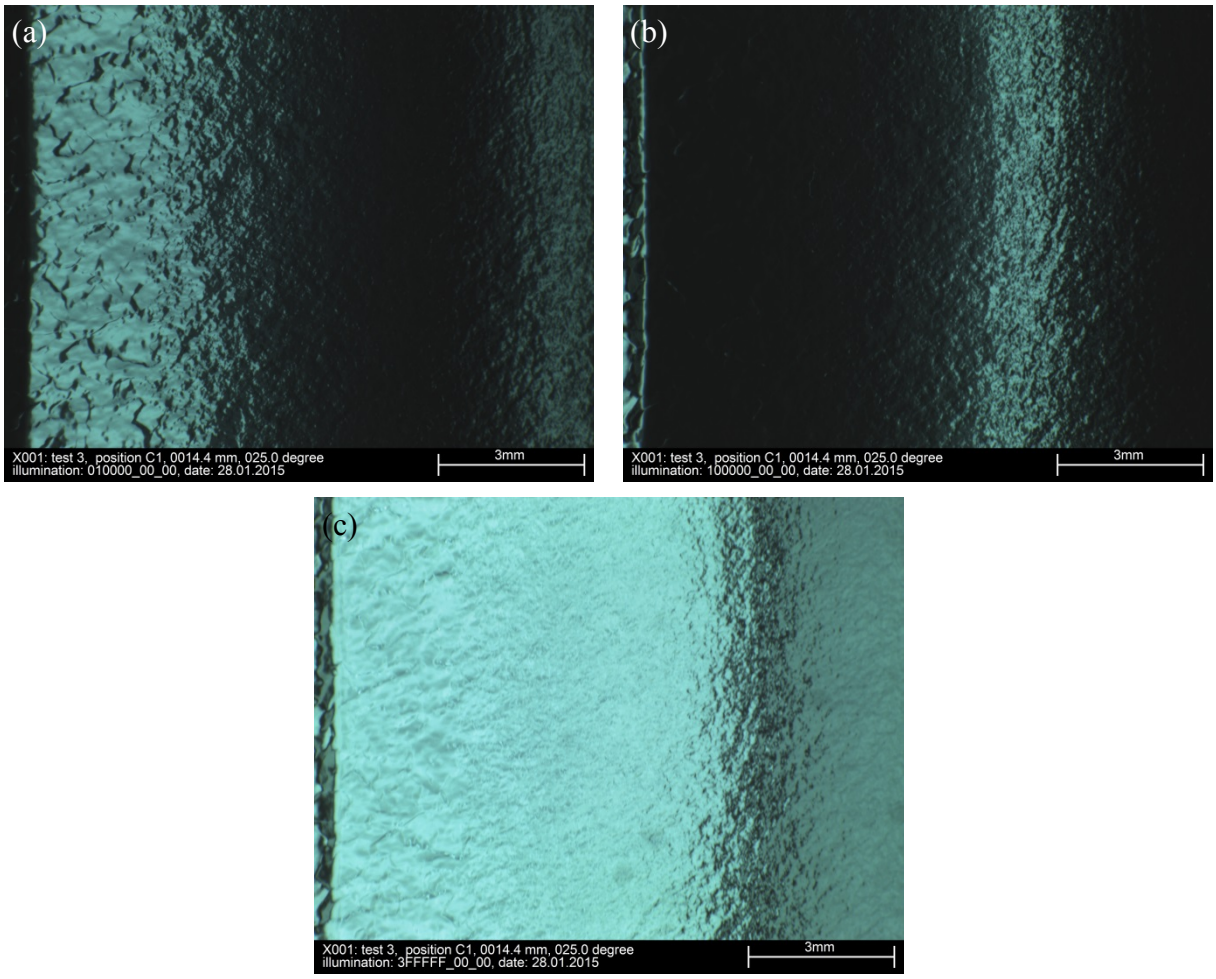

Figure 9: Lighting of a cell with a) strip LED # -6 lit, b) strip LED # -10 lit, and c) all strips enabled.

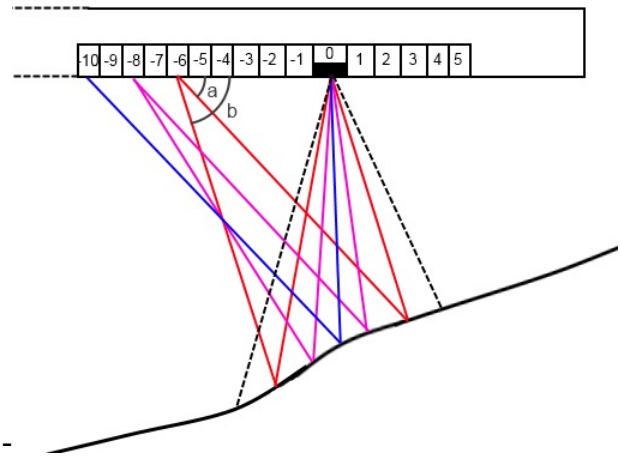

Figure 10: Ray tracing (not to scale) for cavity cell. The camera's field of view (black dashed lines) is only able to see reflections from selected LED strips. Angle *a* is significantly smaller than *b*. Angles and distances have been exaggerated significantly for demonstrative purposes.

The right hand reflected band of each LED is of substantially lower intensity than the left (see figure 9(a)). This is due to (as seen in figure 10) the ray to this location leaving the light strip at a greater angle to the normal, and hence (since emitted intensity is greatest normal to the light strip) being less intense. A dark band remains when all lights are lit (figure 9(c)) since

the two reflections from LED #-10 don't quite meet, meaning this dark section is actually a reflection of the dark and unlit OBACHT boom extending past LED #-10 (to the left of figure 10).

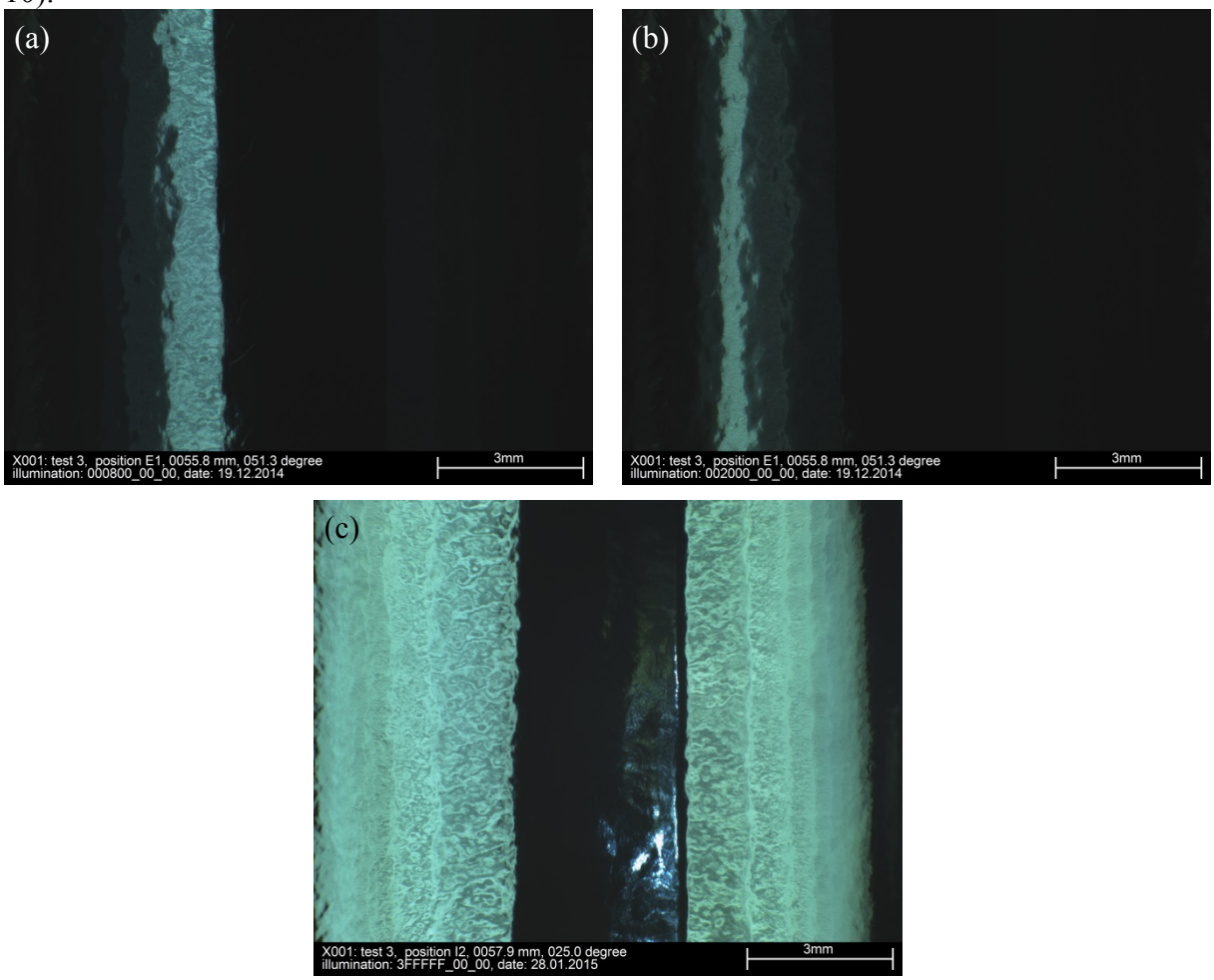

Figure 11: Lighting of Iris from above with a) Strip LED # -1, b) Strip LED # -3, c) All lights enabled.

2.3 Iris Lighting Distribution

Lighting at the Iris is dominated by the peaked nature of the surface. As the depth of the image is significantly greater than the camera's focal depth, only some fraction (either the peak of the iris, or the sides at some distance away) will be in focus. In figure 11 images acquired with an individual light strip, as well as all activated, are demonstrated. It is seen that each light strip provides a single reflection, on the side of the iris it is above, and there is a large unlit zone in the centre. The ray-tracing for this situation is illustrated in figure 12, demonstrating how the band is formed by the camera's imaging its own dark aperture.

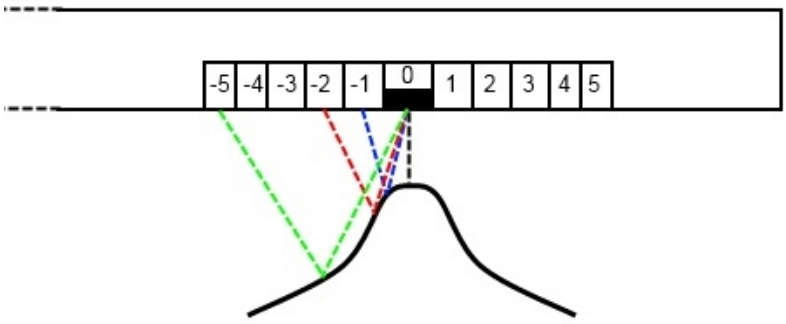

Figure 12: Ray tracing (not to scale) for iris lighting distribution. Individual strip lights are not able to reach the other side of the iris, so only exhibit one reflection, and the central black band is due to the camera's reflection of itself. Geometry of the iris has been exaggerated significantly.

3 Alternative Approaches to Imaging

3.1 Image Combination Algorithm and Filtering

The current best-method for OBACHT lighting is activation of an experimentally determined (so essentially arbitrary) combination of lighting strips, which via visual inspection was found to present good results.
The issue with light selection is that if all lights are activated, uniform lighting over the surface washes out many important features, making identification of defects more difficult. When some light strips are deactivated, the darkness in these bands allows better resolving of fine features, as shadows / highlights are preserved. However, this then produces dark vertical stripes (like those near edges of figure 13) through the image, which could trigger any automated inspection algorithm. So, if possible, we would like to achieve lighting as uniform as possible, whilst maintaining visibility of fine features.
We aim to achieve this by a method for merging of images with different lighting combinations activated. A number of approaches, such as activating light sources individually then combining all pictures, as well as other methods for combination (i.e. activating two strips at a time) have been tested to ascertain how this can best be done. One additional constraint is that of image acquisition efficiency; since the camera takes some not insignificant time to collect each image, we would like to take as few as possible.
After testing, the best compromise was found to be taking two images in which every second light was activated. So, one image is taken with LEDs #[-10, -8, -6, -4, -2, 0, 2, 4, 6, 8, 10, mirror LED] activated, then one with #[-9, -7, -5, -3, -1, 1, 3, 5, 7, 9]. These two images before merging are as in figure 13.

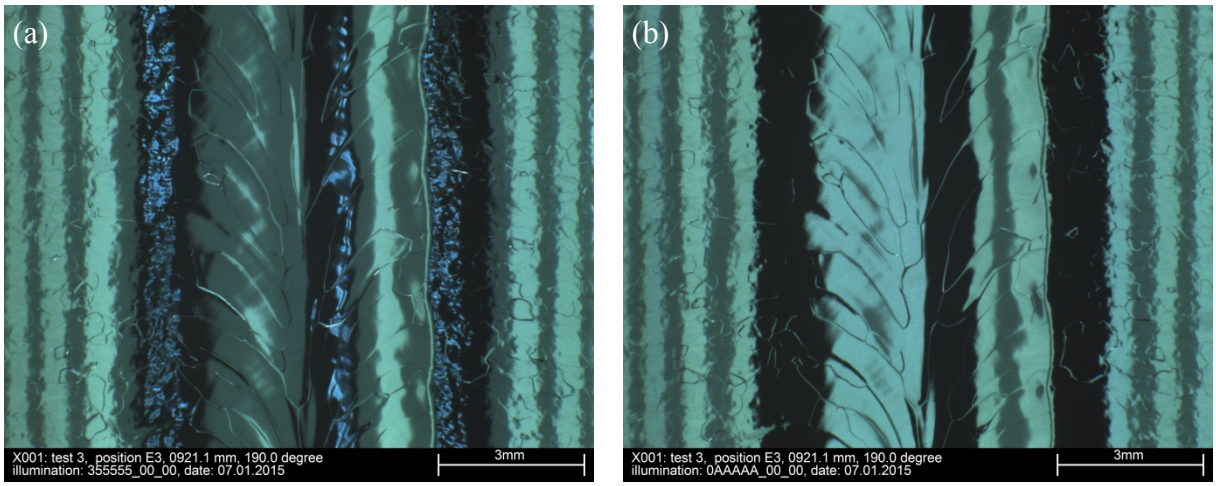

Figure 13: Two images prior to merging: a) image with even lighting, LEDs #[-10, -8, -6, -4, -2, 0, 2, 4, 6, 8, 10, mirror LED], hex code 355555 and b) image with odd lighting, LEDs #[-9, -7, -5, -3, -1, 1, 3, 5, 7, 9], hex code 0AAAAA.

With two images in hand, a method for merging and filtering of the image must be devised. A number of mathematical methods exist, with the following proving to be the most effective approach found.

3.1.1 Image-Merging Algorithm

The image-merging algorithm consists of the following steps:

1. Remove information banner from bottom of each picture. Both images are now 3 layer 8-bit RGB colour images, each consisting of three matrices, one for each colour, with values in the range [0, 255] corresponding to each pixel's intensity.

2. Each colour channel is merged (i.e. image #1 red intensity is combined with image #2 red intensity) by setting the resultant pixel intensities as:

$$I_{x,y,colour} = \left(I^4_{x,y,colour,1} + I^4_{x,y,colour,2}\right)^{0.25},$$

where $I_{x,y,colour,z}$ is the intensity of the pixel representing *colour* (either red, green or blue) at location (x, y) for image z (either image #1 or #2).

3. The resultant image is rescaled to the full 255 bit range. That is, the minimum pixel value is subtracted from the matrix (so the minimum of the matrix is now zero), then the matrix is scaled by element-wise multiplication, such that its maximum value is 255 (i.e. if previous maximum for all colours was 300, multiply whole matrix by 255/300).

3.1.2 Image Filtering Algorithm

Following merging, the image is filtered, with its pixel intensities (for each colour channel) re-scaled. This is done because the initial images have only a few pixels in the high-intensity range ~[200,255], generally corresponding to the few bright spots generated by the central mirror LED's reflection in the dark bands. This forces most of the important features to take place in a limited intensity range (something like ~[60,150] for green and blue channels), which we would like to widen in order to improve contrast in this region.

1. The mean pixel intensities for each channel are recorded:
$I_a = [I_{a,mean,red}, I_{a,mean,green}, I_{a,mean,blue}]$

2. The filter (shown in figure 14) is applied to all layers individually.

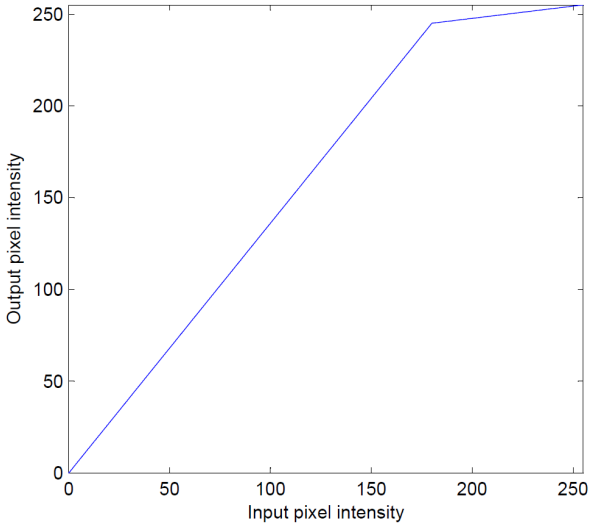

Figure 14: The filter applied to the image re-scales the pixel intensities such that a great range is occupied by regions of interest in the range [60,150]. The turning point (set to input pixel intensity = 180) is chosen via experimentation as it gives good results.

3. In order to maintain relative colour intensities, each colour channel is scaled in order to keep the ratios between mean pixel intensities prior to filtering the same as post-filtering. For this the mean intensities post-filtering are recorded,

$$I_b = [I_{b,mean,red}, I_{b,mean,green}, I_{b,mean,blue}]$$

Then each channel is scaled by:

$$I_{blue} = I_{blue} \times \frac{I_{a,mean,blue}}{\max(I_a)} \times \frac{\max(I_b)}{I_{b,mean,blue}}$$

4. Now filtered (figure 15*)*, each pixel is rounded to the nearest integer to bring the range to [0,255] and the matrices are outputted as a jpg. The information banner is added to the bottom of the image, and each is saved with the new hex code 777777 (to indicate clearly that it is a non-standard lighting setup).

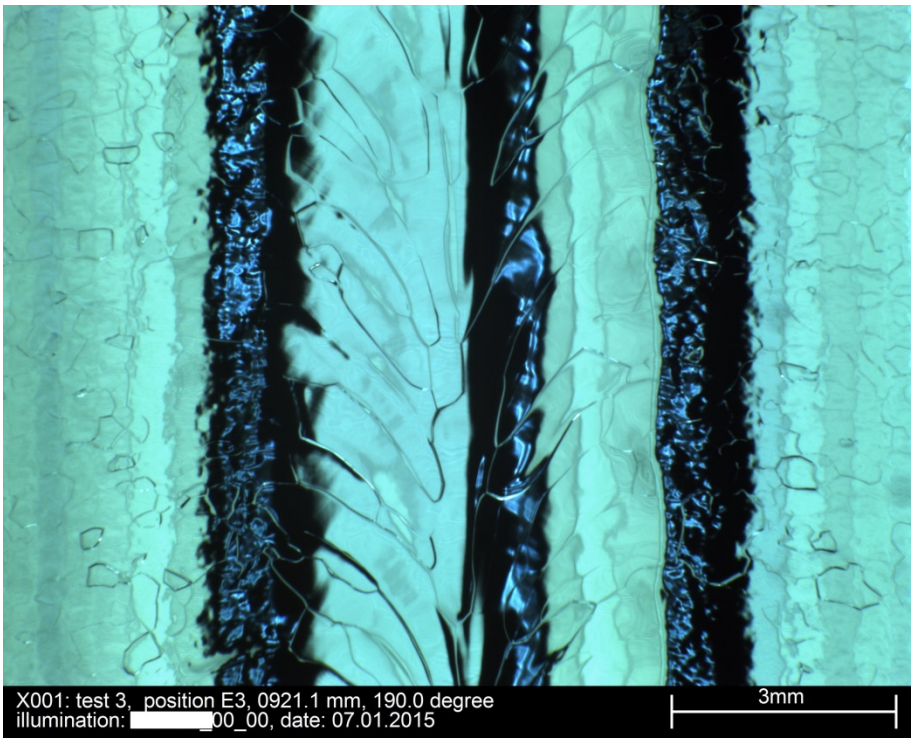

Figure 15: The final combined and filtered image. Compare to figure 3(a) to see how the previously washed-out features when all lights were illuminated are now visible, and figure 3(b) to see how dark vertical bands from the current best lighting setup are minimised.

3.1.3 Other Applications of Image Combination and Filtering

3.1.4 Application to Cell

Applying the algorithm to cell lighting provides some benefit, as the surface is (compared to the iris) relatively flat. This results in more features being resolved, particularly to the equator side of the image (figure 16(a)). However, benefits of the algorithm are not as substantial as for equator imaging, so its implementation may not be performed to reduce the number of images required and hence cavity processing time.

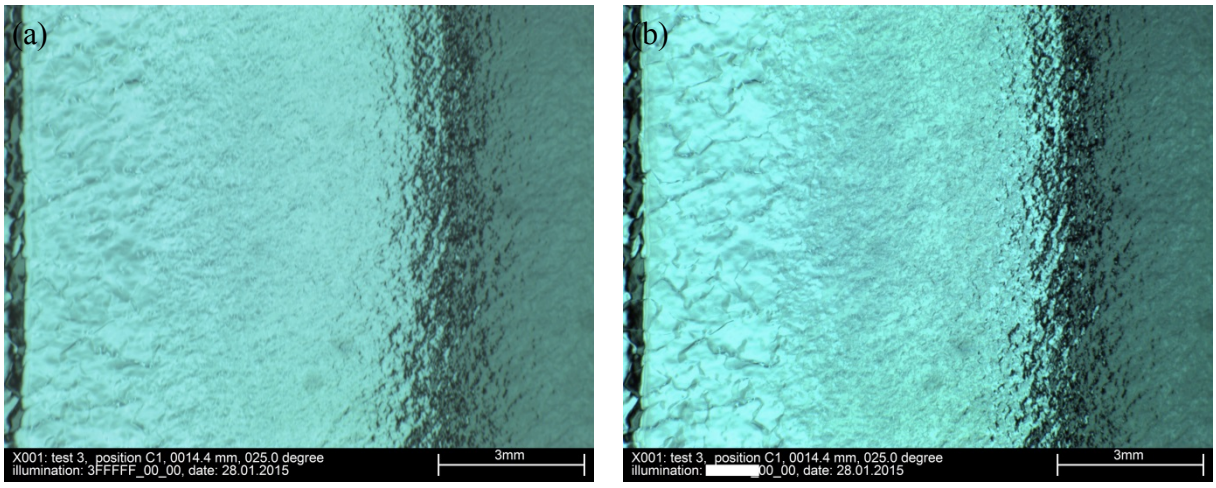

Figure 16: Image of the cell with all lights enabled (a) and image of the same area combined from two images with alternate lighting as per discussed algorithm (b).

3.1.5 Application to Iris

Applying the above algorithm to imaging of the iris provides minimal value, as observed in figure 17. The strength of the algorithm at the equator is that it lights near-flat features first from one direction, then the other, and combines these images to make edges more visible. When we perform the same procedure at the Iris this doesn't take place, since features are on a substantial slope, so all LED's provide light from the same direction. This is more clearly demonstrated in figure 12, where one can see the light from LED's #-1 and #-2 will reach any surface features from the same direction, which is not the case for equator lighting (figure 6) where any feature on the surface between the rays from LED's #-1 and #-2 will be lit from alternate sides.

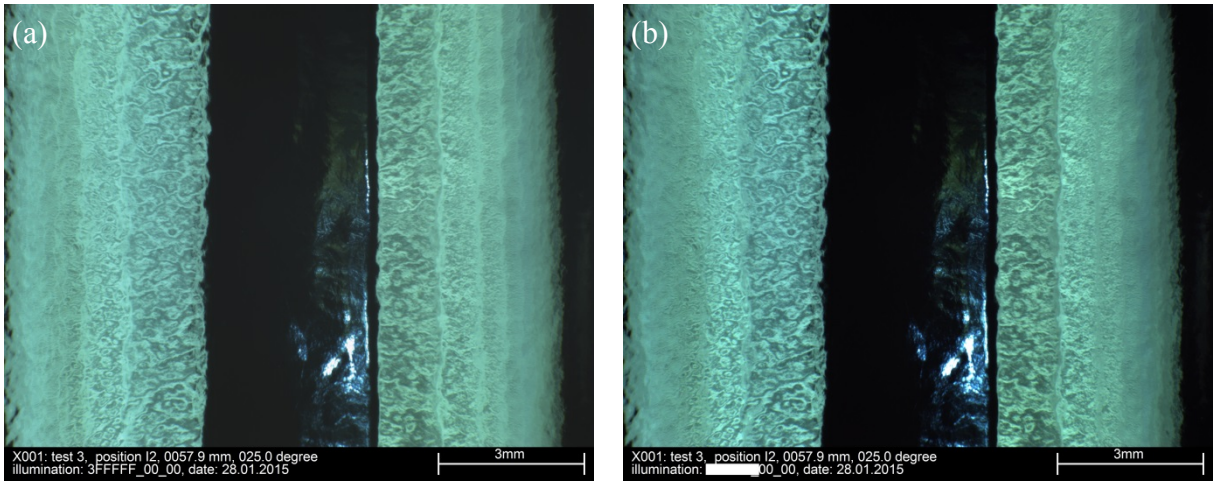

Figure 17: Image of the iris with all lights enabled a) and image of the same area combined from two images with alternate lighting and filtering as per discussed algorithm b). Small differences exist, predominantly due to the filtering process.

3.1.6 Filter Application to Current Equator Lighting

Even without taking multiple images, the filter defined in the algorithm above can be applied in order to enhance the contrast and dynamic range of the image. This is done in figure 18 for an equator image taken using the current best lighting technique, allowing superior viewing of edges and fine details. The image merging process of the algorithm (steps 1 and 2) results in a substantial darkening of the image, which the filter was designed to counteract. In this case, since no combination (and hence darkening) takes place, the filter increases the overall brightness of the image substantially. To see this compare figure 18 with figures 16 & 17, in which the before/after images are of similar brightness

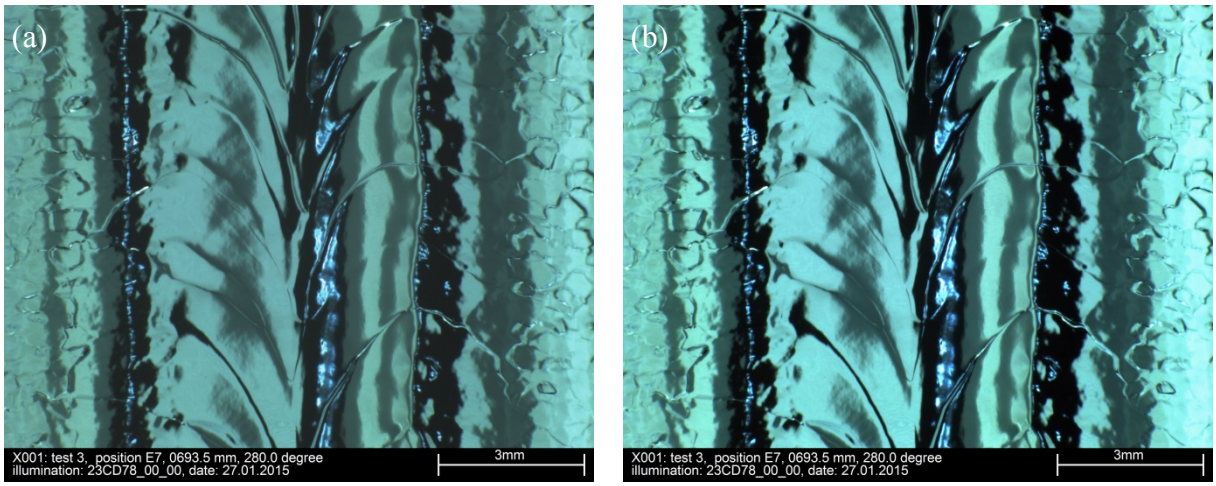

Figure 18: Image of the equator region with the "standard" illumination (hex code 23CD78) a) and filtered image b) as per filtering algorithm outlined above.

3.2 Angled Imaging

Considering the analysis of ray tracing, one approach to an improved lighting uniformity might be imaging different areas of the cell at an angle, such that the reflection of the camera's aperture is minimised or reduced.

3.2.1 Angled Equatorial Imaging

One approach to providing the equator region with consistent lighting is imaging it at an angle, such that the reflection of the camera's lens is not visible. This requires a viewing angle of approximately ±15° to the surface normal, which also necessitates moving the camera approximately 30 mm from its standard position (viewing axis is normal to the surface) to keep the equator in frame and record the same area.

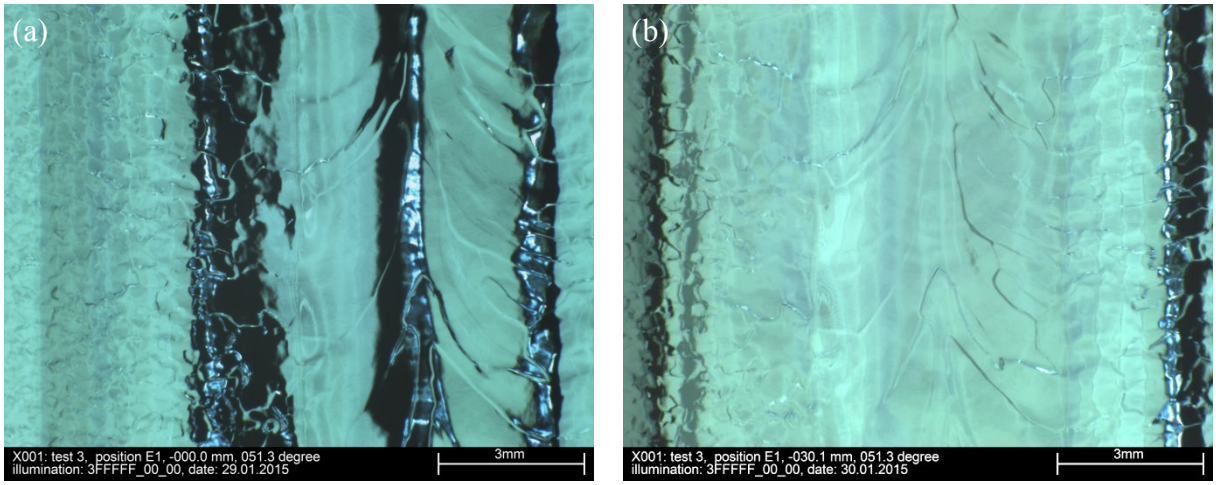

Figure 19: The same cell equator location imaged from a) directly above and b) from an angle of approximately 15°. All illumination is activated. The reflection of the camera lens and three behind-mirror LED's is visible on the right of b), but has been removed from the centre of the welding seam.

In figure 19 this is done with all illumination to moderate success, as the dark bands are now reflected far to the side of welding seam. However, due to imaging at an angle, and the greater distance, the image might be no longer completely in focus, as the camera's depth of field is less or very close to the depth of the features in-frame. Since at this angle the surface is no longer near-planar, 15° tilting of 12 mm planar surface requires around 3 mm depth of field of the camera. This is close to the actual settings of the camera. Furthermore, due to imaging at an angle the welding seam takes up a smaller fraction of the frame, but since the reduction is only around 4%, this should have only a minor impact on the imaging details. Further studies should be done on the illumination in this setup to avoid washing out features as has been done at the equator. Following this, the impact of such imaging on the detectability of defects should be studied as well.
The lighting combination algorithm can be utilised in this situation, however as shown in figure 20 it is not as effective as before; whilst it presents an improvement over the uniform lighting (compare figure 20(c)) with figure 19(b)) it is much easier to make out fine features in the two half-lit images before combination. This is hypothesised to be due to the new angles involved meaning the light reflections occur at an exaggerated angle leading to distorted reflections of the lighting stripes in some regions, which when combined fail to maintain important features.

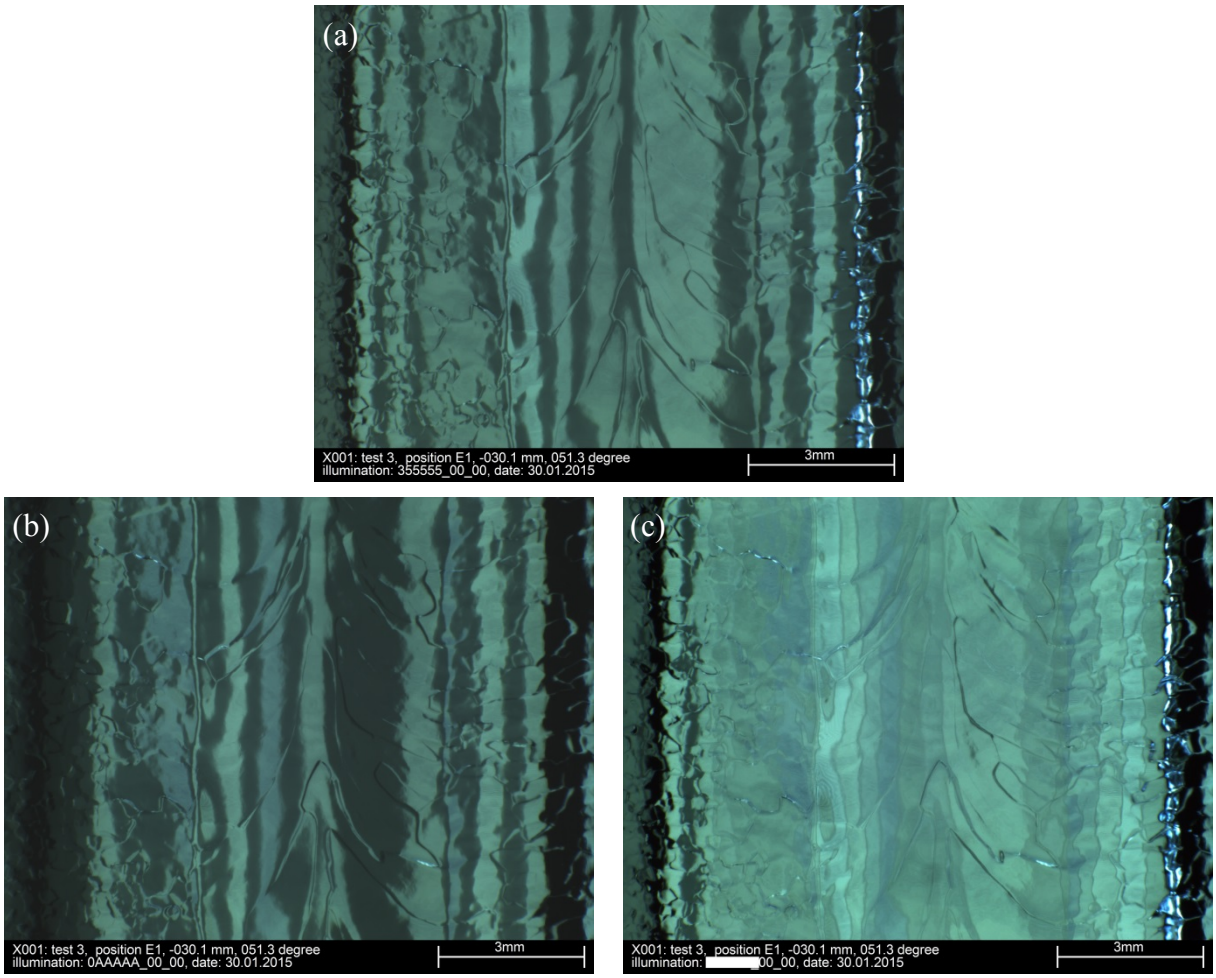

Figure 20: Equator imaged from an angle with alternate lightings a) hex code 355555 and b) hex code 0AAAAA, and c) the result of the combination algorithm and filtering.

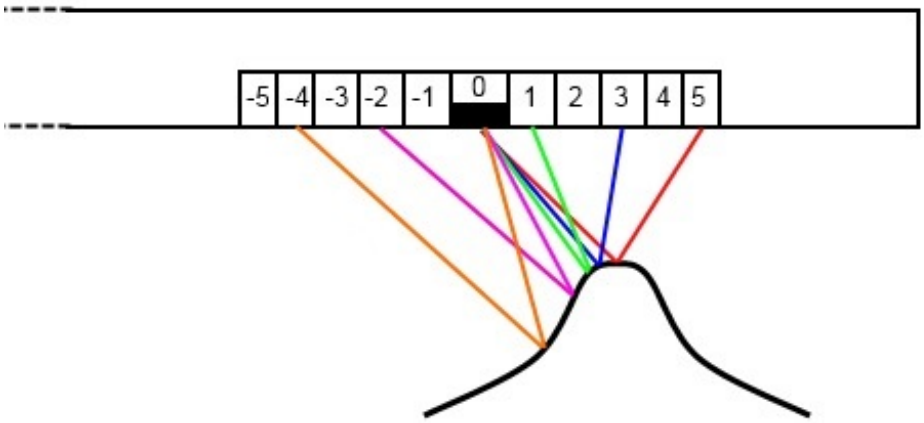

Figure 21: Ray tracing (not to scale) for lighting of iris from an angle of 30°. Correct mirror orientation moves the camera's own reflection off of the iris's peak, allowing better imaging of the welding seam. Geometry of the iris has been exaggerated significantly.

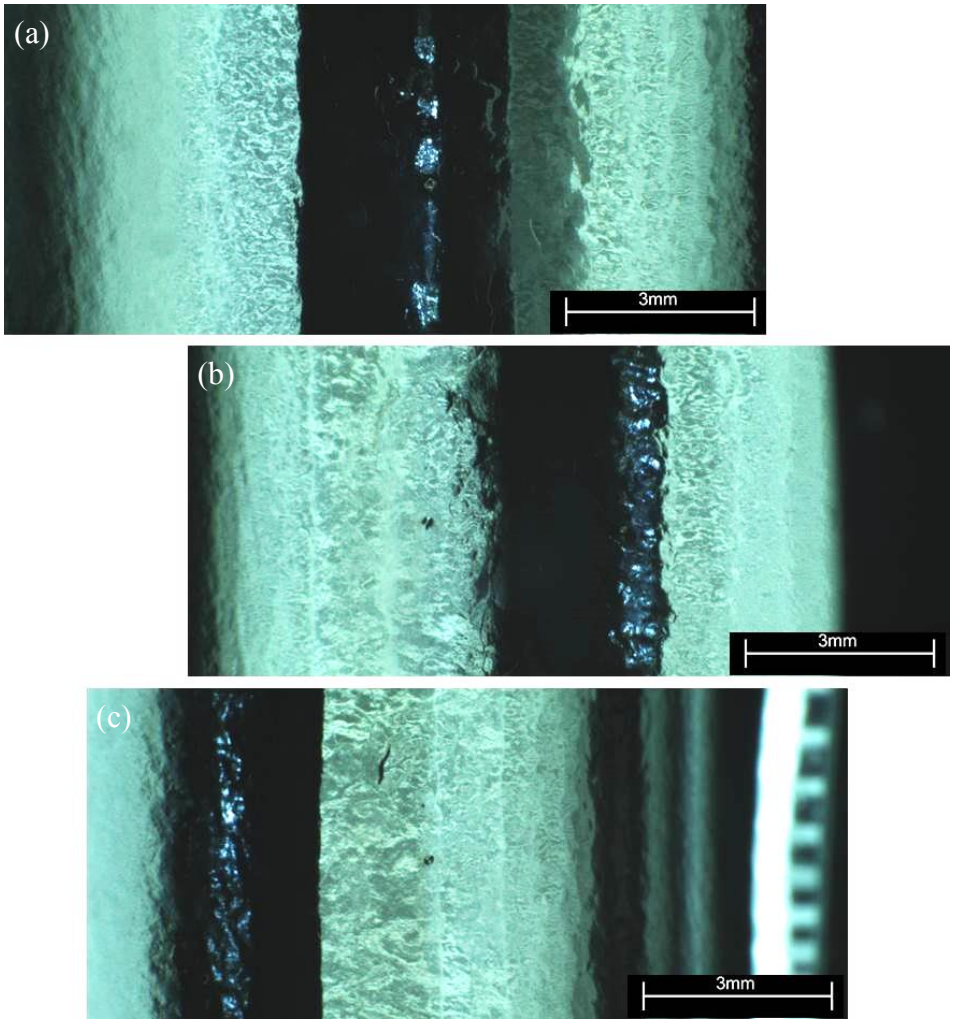

Figure 22: Iris imaged from a) above, b) an angle of approximately +30°, and c) an angle of approximately -30°. Notice the shifted central dark band and fully illuminated and imaged iris welding seam (covered by dark band on a)) with better resolved features, e.g. two visible defects in the middle. The images are shifted to show the same iris location.

3.2.2 Angled Iris Lighting/Imaging

One approach to reducing the Iris's central black line (figure 11(c)) and improving imaging of the surface features is tilting the mirror, such that the iris's welding seam is illuminated and imaged from the side. The ray tracing for this situation is shown in figure 21, where it can be seen the reflection of the camera's aperture moves off of the iris' peak, allowing it to be better lit.

Figure 22 demonstrates this lighting approach, where the reflection of the aperture can be seen to move off of the peak with the substantial viewing angle. The most important area, i.e. the iris welding seam, becomes fully illuminated with better resolved features. For example, two surface defects can be hardly seen on the figure 22(a), whilst imaging with the tilted mirror (figure 22 (c)) allows clear separation of them from the background. The imaging of the whole iris requires, however, at least two images i.e. either both with tilted mirror or one normal to the surface and one tilted. As can be seen in figure 22, the images need to be shifted manually to align the same iris locations, which will be avoided in future by better coupling between the mirror and the camera position. By proper adjustment of the camera position it is possible to further reduce the dark band and allow better resolved features (figure 23), for which an optimum angle and camera position needs to be found via future study.

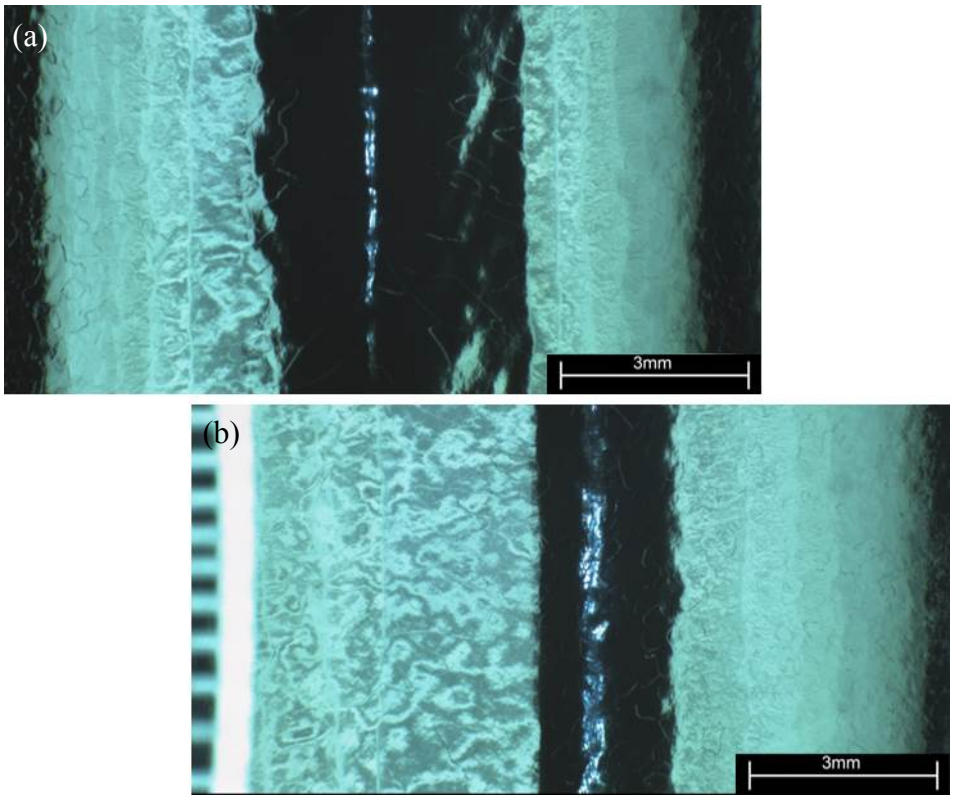

Figure 23: Iris imaged from a) above and b) an angle of approximately 30°. Notice the decreased width of central dark band and better resolved features.

4 Conclusion

Whilst imaging the mirror-like interior of a Niobium superconducting cavity remains difficult, a number of alternatives to the current lighting methodology have been investigated. It is found that equatorial images can be improved substantially, in terms of both features visible and lighting uniformity, via an algorithm which combines and filters two images taken with alternate lighting combinations. Whilst this algorithm does not work as effectively for Iris

imaging, substantial improvements can be realized by imaging the Iris from a significant angle.
With the current machine setup significant improvements on these methods may prove difficult, so if further image enhancements are required then additional light sources, or an improved camera system, will likely be necessary.

References

[1] M. Lemke, et al., "OBACHT - optical bench for automated cavity inspection on short time scales", ILC-HiGrade Report 001, DESY, Hamburg, Germany, 2013.
[2] A. Navitski, E. Elsen, B. Foster, R. Laasch, D. Reschke, J. Schaffran, W. Singer, X. Singer, Y. Tamashevich, "R&D on cavity treatments at DESY towards the ILC performance goal," Proceedings of 16th International Conference on RF Superconductivity, SRF 2013, Sep. 23-27, Paris, France, MOP053, p. 240-243, ISBN 978-3-95450-143-4 (2013).

Appendix

The following is a MATLAB (.m) code which, when run in a directory containing images taken using the lighting-combination feature of the OBACHT inspection (i.e. locations have images with lighting hex codes #355555 and 0AAAAA), will perform the combination and filtering process on all possible images in that folder, and write new images with filename hex codes #777777. To use it just copy all code into MATLAB, save the .m file in the directory containing images, and click run.
A sub-code to generate these images, two images of the appropriate lighting at each equatorial location, in a Cavity has already been integrated into the LabVIEW automated inspection software.

```
clear
clc
clf

lighting1='0AAAAA';
lighting2='355555';
output_hex='777777';
%Now we are going to compile a list of the files which need to be examined
list=ls;
list2=[];
%Here we sort out just the images and make a list
for i=1:size(list,1)
    rowint=list(i,:);
    present=strfind(rowint,'jpg');
    if sum(size(present))>1
        list2=[list2;rowint];

    end
end
list3=cell(0);
count=1;

%Now we go on to sort out only the ones with appropriate lighting which
%need to be combined, and group them together.
location=1;
count1=1;
list2a=cell(0);
while location<size(list2,1)
    flag=0;
```

```
    to_add=list2(location,:);
    count2=1;
    while flag==0

        tf=strcmp(list2(location,1:23),list2(location+count2,1:23));
        if tf
            to_add=[to_add;list2(location+count2,:)];
            count2=count2+1;
        else
            flag=1;
        end
        if location+count2>size(list2,1)
            flag=1;
        end
    end
    location=location+count2;
    list2a{1,count1}=[to_add];
    count1=count1+1;
end

loc=1;
for i=1:size(list2a,2)
   int=list2a{i};
   int2=int(:,24:29);
   vals1a=[ismember(int2,lighting1)];
   vals1b=[ismember(int2,lighting2)];
   vals2a=(sum(vals1a')==6);
   vals2b=(sum(vals1b')==6);
   loc1a=find(vals2a==1);
   loc1b=find(vals2b==1);
   check1=sum(size(loc1a));
   check2=sum(size(loc1b));
   if and(check1==1,check2==1);
      disp(['Didnt take multiple-lighting pictures at: ',int(1,1:23)])
   elseif or(check1==1,check2==1);
       disp(['Missing second lighting combination at: ',int(1,1:23)])
   elseif or (check1>2,check2>2);
       disp(['Some mixup occured at location: ',int(1,1:23)])
   else
       list3{1,loc}=[int(loc1a,:);int(loc1b,:)];
       loc=loc+1;
   end
end

%Now we will process each picture and save the new file;
maxval=size(list3,2);
fprintf('Minutes remaining:  0060.00')
time=0;
for ir=1:maxval
    tic
    pics=list3{ir};

      ima=imread(pics(1,:));
      left=(ima(1:2616,1:3488,1:3));
      ima=imread(pics(2,:));
      right=(ima(1:2616,1:3488,1:3));

      comb=0*double(right);
      n=4;
      for i=1:3
```

```
            c=((double(left(:,:,i)).^n+double(right(:,:,i)).^n).^(1/n));
            c=c-min(min(c));
            comb(:,:,i)=(c);
        end
        comb=comb*255/max(max(max(comb)));
        relative_mag=mean(mean(comb));
        for i=1:3
            c=comb(:,:,i);
            %Linear FIlter
            a=180;
            m1=(245/a);
            m2=10/(255-a);
            b2=245-a*m2;
            sel=c<=a;
            y=(sel).*(m1*c)+(1-sel).*(m2*c+b2);
            comb(:,:,i)=y;
        end
        relative_mag2=mean(mean(comb));
        max1=max(relative_mag);
        max2=max(relative_mag2);
        Ratio=(relative_mag./relative_mag2)*max2/max1;
        for i=1:3
            comb(:,:,i)=comb(:,:,i)*Ratio(i);
        end

        combined_lr=uint8(comb);

        ima(1:2616,1:3488,1:3)=combined_lr;
        ima(2715:2780,490:805,:)=255;
        name=pics(1,:);
        name(24:29)=output_hex;
        imwrite(ima,name,'jpg')
        b=toc;
        time=time+b;
        time_remain=(maxval-ir)*(time/ir)/60;
        str=num2str(time_remain,3);
        while length(str)<5
            str=['0' str];
        end

        fprintf('\b\b\b\b\b\b%s\n',str)

end
```